Dalton
www.rsc.org/dalton

4,6-Dihydroxypyrimidine: a selective bridging ligand for controlled Group IV metal alkoxide structures

Timothy J. Boyle,* Mark A. Rodriguez and Todd M. Alam
Advanced Materials Laboratory, Sandia National Laboratories, 1001 University Boulevard, SE, Albuquerque, NM 87106, USA. E-mail: tjboyle@Sandia.gov

Received 21st August 2003, Accepted 17th October 2003
First published as an Advance Article on the web 31st October 2003

The generation of controlled metal alkoxide structures has been explored using 4,6-dihydroxypyrimidine (DHP-H_2) as a selective bridging ligand. DHP-H_2 was reacted with $Ti(OPr^i)_4$ in pyridine (py). Crystallization from this solution led to the isolation of $[(OPr^i)_2(\mu\text{-}OPr^i)Ti(\mu\text{-}DHP)Ti(OPr^i)_3(py)]_2$ (**1**). The two dinuclear subunits of **1** possess a bridging DHP ligand bound through both the O and N of the ring, forming an M–O–C–N ring on each metal center. The first Ti possesses three terminal OR ligands and one coordinated pyridine solvent molecule. The second Ti is connected to a μ-OPr^i group from the other subunit, forming a tetranuclear species. In contrast, recrystallization of **1** from toluene provided the solvent-free, cyclic adduct $\{[(OPr^i)_2(\mu\text{-}OPr^i)Ti]_2(\mu\text{-}DHP)\}_2$ (**2**). An identical reaction using more sterically hindering alkoxy precursors yielded products of the general structure $[(py)(RO)_3M]_2(\mu_4\text{-}DHP)$, where M = Ti, OR = OCH_2CMe_3 (**3**), $OPr^i/OCMe_3$ (**4**); M = Zr, OR = $OCMe_3$ (**5**). Each metal center adopts an octahedral geometry, with one py, three terminal alkoxide ligands, and one bridging DHP. Solid-state ^{13}C MAS NMR studies indicate the bulk materials are consistent with the crystal structures and solution ^1H NMR is consistent with retention of the structures in solution for **2**–**5**.

Introduction

Metal alkoxides $[M(OR)_x]$ have found great utility as precursors in solution (*i.e.*, sol–gel) or gaseous (*i.e.*, metallo-organic vapor deposition) routes to thin films of ceramic materials.[1–5] It has been reported that the characteristics of $M(OR)_4$ precursors greatly affect the final properties of the resultant ceramic materials.[1–9] This is mainly a result of changes in the hydrolysis and condensation rates of the $M(OR)_4$ as influenced by the number and types of ligands present. For instance, controlling the number of terminal alkoxides present in a series of carboxylic acid-modified titanium alkoxides was shown to directly influence the degree of densification for thin films of anatase.[9] Hence, selectively manipulating the structure of the starting $M(OR)_4$ is very important in the generation of tailor-made ceramic materials.

However, rational construction of $M(OR)_x$ is an ongoing challenge, mainly due the large cation size to charge ratio which leads to the oligomerization, oxo formation, and/or inclusion of unexpected ions. One method that is employed to circumvent this problem is to utilize large, sterically bulky ligands to reduce the degree of oligomerization by blocking open coordination sites. However, this method often leads to monomeric species and this greatly limits the ability to generate the structural variations necessary to impart control over the properties of the final ceramic materials of interest.

Nevertheless, it may be possible to exploit the oligomeric nature of metal alkoxides if a ligand that preferentially acts as a bridge is employed. By controlling the number of bridging ligands, we envision the construction of predictable, tailored $M(OR)_x$ species (see Scheme 1). This approach has been previously employed to generate controlled metal amide species using electronic variations of the N-bearing ligands,[10] but that method cannot be used for alkoxide ligands, since the electronic nature of the oxygen atom is not as flexible as the N of the amide system. Therefore, we investigated sterically rigid, appropriately oriented, polydentate alcohols. Several potential ligands were considered, but the geometrical constraints of 4,6-dihydroxypyrimidine (DHP-H_2; eqn. 1) offered the greatest opportunity to generate the structures presented in Scheme 1. We envision the use of the DHP bridging ligand as a means of generating dinuclear 'building blocks' that can be systematically reacted to assemble structures of interest. Scheme 1 shows some of the general structures arising from this concept of building

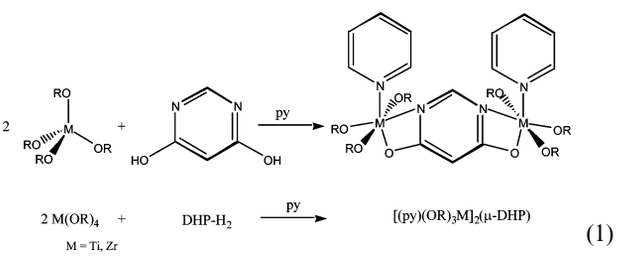

(1)

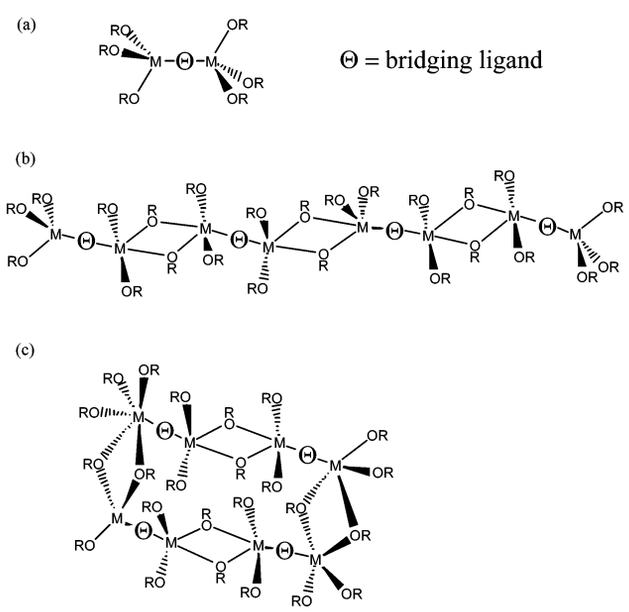

Scheme 1 Rational construction of metal alkoxides: (a) dimer (beginning scaffold); (b) polymer chain (length determined by number of bridging ligands); (c) rings. OR = alkoxide ligand, Θ = bridging ligand.

controlled dimers, oligomers, rings, *etc*., to ultimately control the properties of the final ceramic materials.

Group IV species were selected for this initial study due to their ubiquity in ceramic materials. From the reaction of $M(OR)_4$ (M = Ti, Zr) with DHP-H_2 in pyridine (py; eqn. 1), the following products were isolated, $[(py)(OPr^i)_3Ti(\mu\text{-}DHP)\text{-}Ti(\mu\text{-}OPr^i)(OPr^i)_2]_2$ (**1**), $\{[(OPr^i)_2(\mu\text{-}OPr^i)Ti]_2(\mu\text{-}DHP)\}_2$ (**2a**, **b**),

DOI: 10.1039/b310087a

 This journal is © The Royal Society of Chemistry 2003

$[(py)(ONep)_3Ti]_2(\mu_4\text{-DHP})$ (**3**; ONep = OCH_2CMe_3), $[(OPr^i)_x(OBu^t)_y(py)Ti]_2(\mu\text{-DHP})$ (**4a**, $x = 2$, $y = 1$; **4b**, $x = 3$, $y = 3$), $[(py)(OBu^t)_3Zr]_2(\mu_4\text{-DHP})$ (**5**), and are shown in Fig. 1–5, respectively. The synthesis and structural properties of these compounds are described in detail in this report.

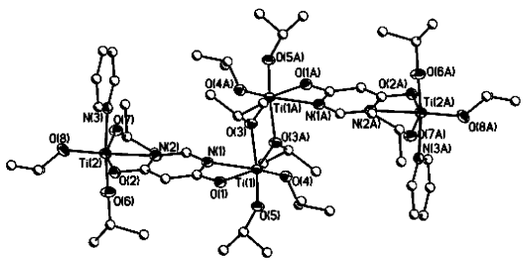

Fig. 1 Thermal ellipsoid plot of **1**. Thermal ellipsoids are drawn at the 30% probability level.

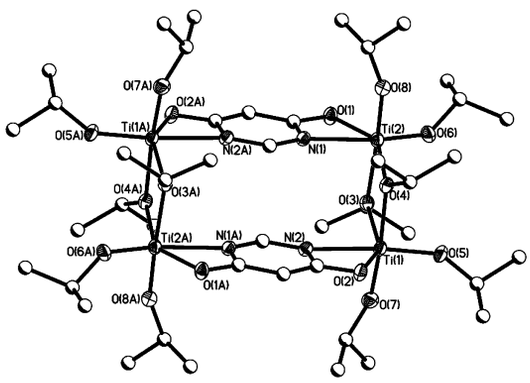

Fig. 2 Thermal ellipsoid plot of **2b**. Thermal ellipsoids are drawn at the 30% probability level.

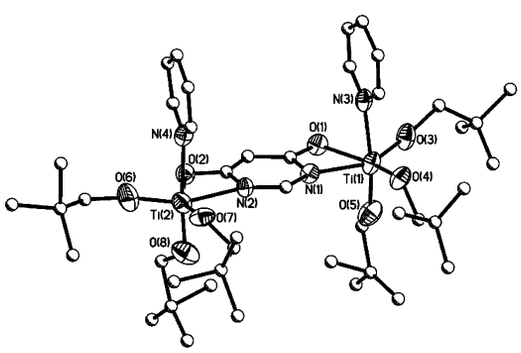

Fig. 3 Thermal ellipsoid plot of **3**. Thermal ellipsoids are drawn at the 30% probability level.

Experimental

All compounds described below were handled with rigorous exclusion of air and water using standard Schlenk line and glove box techniques. FT-IR data were obtained with a Bruker Vector 22 spectrometer using KBr pellets under an atmosphere of flowing nitrogen. Elemental analyses were performed using a Perkin-Elmer 2400 CHN-S/O elemental analyzer. The following chemicals were used as received (Aldrich), stored, and handled under an argon atmosphere: pyridine (in a Sureseal bottle), H-ONep, DHP-H_2, $Ti(OPr^i)_4$, $Ti(OBu^t)_4$, and $Zr(OBu^t)_4$. $[Ti(\mu\text{-ONep})(ONep)_3]_2$ [11] was synthesized from the reaction of $Ti(OPr^i)_4$ and HONep as previously reported.

Synthesis

The preparation processes for compounds **1**–**5** are very similar, hence, a general procedure is given here and any particular variations are noted in the individual sections below. Under an argon atmosphere, DHP-H_2 was added to $M(OR)_4$ dissolved in toluene and the resulting yellow slurry was stirred for 5 min. Then, pyridine was added and the reaction mixture was heated until it became clear. The solution was stirred overnight. X-Ray quality crystals were grown at ambient glovebox temperatures by slow evaporation of the volatile material from each sample.

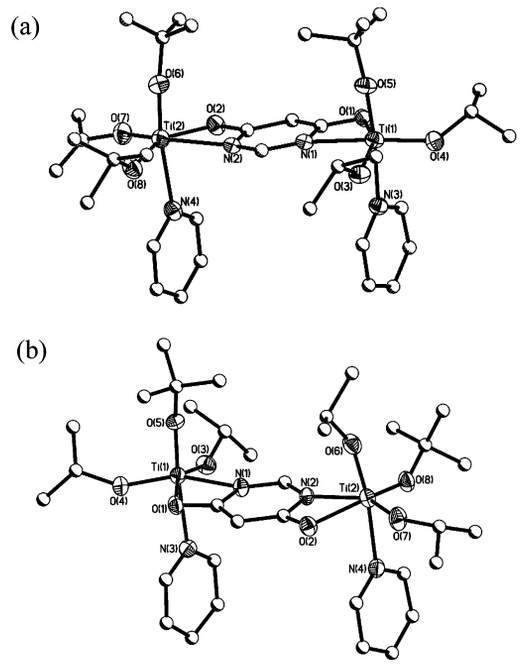

Fig. 4 Thermal ellipsoid plots of **4a** and **4b**: (a) isolated from the '$Ti(OBu^t)_x(OPr^i)_{4-x}$' mixture received from Chemat; (b) isolated from the 50 : 50 mixture of '$Ti(OBu^t)_2(OPr^i)_2$'. Thermal ellipsoids are drawn at the 30% probability level. The ligands were arbitrarily chosen based on electron density maps.

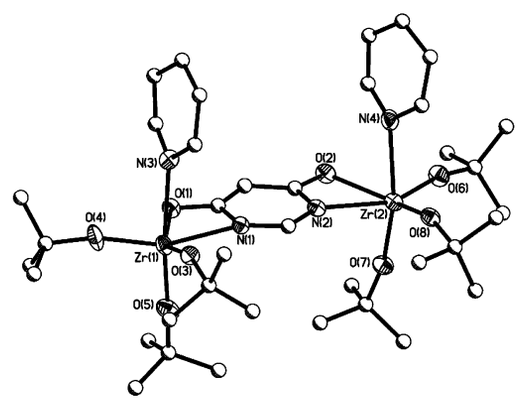

Fig. 5 Thermal ellipsoid plot of **5**. Thermal ellipsoids are drawn at the 30% probability level.

$[(py)(OPr^i)_3Ti(\mu\text{-DHP})Ti(\mu\text{-}OPr^i)(OPr^i)_2]_2$ (1). Used $Ti(OPr^i)_4$ (1.00 g, 3.52 mmol) and DHP-H_2 (0.197 g, 1.76 mmol) in toluene (2 mL) and py (10 mL). Yield 80% (0.90 g). FTIR (KBr) ν/cm^{-1}: 2967(s), 2931(m), 2863(m), 1609(s), 1478(s), 1442(m), 1383(w), 1360(w), 1329(w), 1243(m), 1206(s), 1166(s), 1126(s), 1020(s), 982(s), 852(m), 823(m), 635(s), 603, 465(m). ^{1}H NMR (399.8 MHz, py-d_5): δ 8.41 (1.4H, s, $C_4N_2O_2H_2$), 5.44 (0.19H, s, $C_4N_2O_2H_2$), 5.00 [10.3H, s(br), $OCH(CH_3)_2$], 1.31 [78H, d, $OCH(CH_3)_2$, J_{H-H} = 6 Hz]. Elemental analysis calc'd for $C_{54}H_{98}N_6O_{16}Ti_4$: C 50.71, H 7.72, N 6.57; found: C 50.25, H 7.49, N 6.50%.

$\{[(OPr^i)_2(\mu\text{-}OPr^i)Ti]_2(\mu\text{-DHP})\}_2$ (2). Used $Ti(OPr^i)_4$ (1.00 g, 3.52 mmol) and DHP-H_2 (0.197 g, 1.76 mmol) in toluene (2 mL) and py (10 mL). The solvent was evaporated *in vacuo*

and the residue redissolved in hot toluene; crystals were isolated as the solution cooled. Yield 72% (0.71 g). FTIR (KBr) ν/cm^{-1}: 2966(s), 2932(m), 2862(m), 1612(s), 1481(s), 1377(s), 1360(m), 1324(m), 1241(m), 1166(s), 1136(s), 1114(s), 1017(s), 991(s), 936(m), 853(m), 822(m), 623(w), 591, 567(m). ^{1}H NMR (399.8 MHz, py-d_5): δ 7.02 (0.5H, s, $C_4N_2O_2H_2$), 5.47 (0.5H, s, $C_4N_2O_2H_2$), 5.29, 5.17, 4.59 [each 1.6H, 3 × sept, OCH(CH$_3$)$_2$, J_{H-H} = 3.2 Hz], 1.66, 1.45, 1.35, 1.30, 1.20, 1.15 [each 4.6H, 6 × d, OCH(CH_3)$_2$, J_{H-H} = 3.2 Hz]. ^{13}C{^{1}H} (100.6 MHz, py-d_5): δ 178.4, 150.2, 83.7 ($C_4N_2O_2H_2$), 81.0, 79.5, 75.5 [OCH(CH$_3$)$_2$] 26.2, 25.8, 25.7, 25.4, 24.7, 24.4 [OCH(CH$_3$)$_3$]. Elemental analysis calc'd for $C_{44}H_{86}N_4O_{16}Ti_4$: C 47.23, H 7.74, N 5.01; found: C 47.31, H 8.13, N 4.96%.

[(py)(ONep)$_3$Ti]$_2$(μ_4-DHP) (3). Used [Ti(ONep)$_4$]$_2$ (1.00 g, 2.53 mmol) and DHP-H$_2$ (0.141 g, 1.26 mmol) in toluene (2 mL) and py (10 mL). Yield: 91% (0.83 g). FTIR (KBr) ν/cm^{-1}: 2953(s), 2866(m), 2827(m), 1609(s), 1480(m), 1442(m), 1392(w), 1362(w), 1253(w), 1060(s), 1023(m), 821(w), 755(w), 702(s, sh), 673(s). ^{1}H NMR (399.8 MHz, py-d_5): δ 8.80 (1.0H, s, $C_4N_2O_2H_2$), 5.80 (1.3H, s, $C_4N_2O_2H_2$), 4.55 [18H, s, OCH_2C(CH$_3$)$_3$], 1.24 [87H, s, OCH$_2$C(CH_3)$_3$]. Elemental analysis calc'd for $C_{44}H_{78}N_4O_8Ti_2$: C 59.58, H 8.86, N 6.31; found: C 59.04, H 8.51, N 6.09%.

[(py)(OPr^i)$_4$(OBu^t)$_2$Ti]$_2$(μ_4-DHP) (4). 'Ti(OBu^t)$_2$(OPr^i)$_2$' was synthesized from an equimolar mixture of Ti(OBu^t)$_4$ and Ti(OPr^i)$_4$. Used 'Ti(OBu^t)$_2$(OPr^i)$_2$' (1.00 g, 3.21 mmol) and DHP-H$_2$ (0.165 g, 1.47 mmol) in toluene (2 mL) and py (10 mL). Yield 67% (0.80 g). FTIR (KBr) ν/cm^{-1}: 2969(s), 2927(m), 2863(m), 1603(s), 1479(s), 1445(m), 1377(w), 1359(w), 1325(w), 1246(w), 1192(w), 1164(m), 1126(m), 1114(s), 1009(w), 982(w), 852(w), 822(w), 692(m), 611(m), 575(m). ^{1}H NMR (399.8 MHz, py-d_5): δ 8.37 [0.6H, s(br), $C_4N_2O_2H_2$], 5.0 [5H, s(br), OCH-(CH$_3$)$_2$], 1.40 [24H, s, OC(CH$_3$)$_3$], 1.29 [48H, d, OCH(CH_3)$_2$, J_{H-H} = 3.6 Hz]. Elemental analysis calc'd for $C_{34}H_{46}N_4O_9Ti_2$: C 55.59, H 6.31, N 7.63; found: C 54.33, H 7.64, N 7.07%.

[(py)(OBu^t)$_3$Zr]$_2$(μ_4-DHP) (5). Used Zr(OBu^t)$_4$ (1.00 g, 2.61 mmol) and DHP-H$_2$ (0.146 g,1.30 mmol) in toluene (2 mL) and py (10 mL). Yield 77% (0.89 g). FTIR (KBr) ν/cm^{-1}: 2968(s), 2924(m), 2863(m), 1615(s), 1488(m), 1441(m), 1382(m), 1357(m), 1259(m), 1231(s, sh), 1210(s), 1191(s), 1043(m), 995(s), 784(m), 700(m), 534(s). ^{1}H NMR (399.8 MHz, py-d_5): δ 8.13 (1H, s, $C_4N_2O_2H_2$), 5.71 (0.71H, s, $C_4N_2O_2H_2$), 1.36 [83.6H, s, OC(CH$_3$)$_3$]. Elemental analysis calc'd for $C_{38}H_{66}N_4O_8Zr_2$: C 51.32, H 7.48, N 6.30; found: C 50.40, H 7.07, N 6.13%.

NMR spectroscopy

The solid-state MAS NMR spectra were obtained with a Bruker Avance instrument using a 4 mm bb probe. The ^{13}C CP-MAS spectra were obtained at 100.6 MHz using a 1 ms contact time, 64–128 scans, spinning speeds between 4 and 10 kHz, and 10 s recycle delay with high power ^{1}H TPPM decoupling. The high resolution ^{1}H and ^{13}C NMR spectra were obtained at 399.8 and 100.6 MHz, respectively, with a Bruker DRX400 instrument using a 5 mm broad-band probe. Standard pulse sequences were used in all cases. The ^{1}H and ^{13}C spectra were referenced to the deuterated solvent signal.

X-Ray crystallography

Table 1 list the data collection parameters for **1**, **2a**, **b**, and **3**–**5**, respectively. Metrical data for all compounds can be found in the CIFs (see below). All crystals were mounted onto a thin glass fiber from a pool of Fluorolube™ and placed immediately under a liquid N$_2$ stream on a Bruker AXS diffractometer. Structural solutions were performed using the following software: SMART version 5.054, SAINT+ 6.02 (7/13/99),

Table 1 Data collection parameters for **1**–**5**

	1	**2a**	**2b**	**3**	**4a**	**4b**	**5**
Chemical formula	$C_{54}H_{98}N_6O_{16}Ti_4$	$C_{44}H_{86}N_4O_{16}Ti_4$	$C_{44}H_{88}N_4O_{16}Ti_4$	$C_{44}H_{39}N_4O_8Ti_2$	$C_{32}H_{56}N_4O_8Ti_2$	$C_{34}H_{46}N_4O_8Ti_2$	$C_{36}H_{66}N_4O_8Zr_2$
Formula weight	1278.98	1120.78	1120.78	847.59	720.61	734.55	889.39
T/K	168(2)	168(2)	168(2)	168(2)	168(2)	168(2)	168(2)
Crystal system, space group	Triclinic, $P\bar{1}$	Monoclinic, $P2(1)/n$	Triclinic, $P\bar{1}$	Triclinic, $P\bar{1}$	Monoclinic, $P2(1)/n$	Monoclinic, $P2(1)/n$	Monoclinic, $P2(1)/n$
a/Å	10.787(3)	16.361(3)	11.732(5)	10.250(7)	9.5723(12)	9.6835(12)	16.757(13)
b/Å	11.751(3)	9.3285(18)	15.003(6)	16.064(12)	18.416(2)	16.271(2)	9.969(7)
c/Å	13.251(3)	21.262(4)	17.776(7)	16.906(12)	24.619(3)	27.414(3)	28.15(2)
α/°	90.901(4)		96.204(6)	71.802(13)			
β/°	91.650(4)	106.721(4)	98.401(6)	86.040(16)	101.200(3)	95.913(3)	91.761(15)
γ/°	92.000(4)		103.870(6)	88.807(14)			
V/Å^3	1677.7(7)	3107.9(10)	2972(2)	2638(3)	4257.2(9)	4296.4(9)	4701(6)
Z	1	2	2	2	4	4	4
D_{calcd}/Mg m^{-3}	1.266	1.196	1.253	1.067	1.124	1.136	1.257
μ(Mo-Kα)/mm^{-1}	0.522	0.553	0.579	0.348	0.419	0.417	0.490
$R1$ [a] (%) (all data)	6.05 (9.00)	8.38 (15.16)	5.94 (7.69)	10.51 (27.43)	9.34 (26.57)	12.51 (18.23)	6.33 (12.71)
$wR2$ [b] (%) (all data)	17.75 (19.83)	22.41 (27.50)	14.49 (15.55)	19.39 (33.27)	14.62 (30.76)	35.45 (38.87)	11.60 (14.67)

[a] $R1 = \Sigma||F_o| - |F_c||/\Sigma|F_o| \times 100$. [b] $wR2 = [\Sigma w(F_o^2 - F_c^2)^2/\Sigma(w|F_o^2|^2)]^{1/2} \times 100$ for $[I < 2\sigma(I)]$.

SHELXTL 5.1 (10/29/98), XSHELL 4.1 (11/08/00), and SADABS within the SAINT+ package.[12] Each structure was solved using direct methods, yielding the metal center, O, N, and some of the C atoms, with subsequent Fourier synthesis yielding the remaining C atom positions. The hydrogen atoms were fixed in positions of ideal geometry and refined within the XSHELL software. These idealized hydrogen atoms had their isotropic temperature factors fixed at 1.2 or 1.5 times the equivalent isotropic *U* of the C atoms to which they were bonded. The final refinement of each compound included anisotropic thermal parameters on all non-hydrogen atoms, unless otherwise noted below. See Table 1 or CIFs for additional details.

For the following compounds, if any H atoms were removed during refinement due to disorder, the proper number of H atoms were included in the formula in the final refinement to calculate the proper crystallographic data. Complete convergence for each of these compounds was not possible due to disorder in the pendant chains of the alkoxide.

CCDC reference numbers 218027–218033.

See http://www.rsc.org/suppdata/dt/b3/b310087a/ for crystallographic data in CIF or other electronic format.

Compound 1. O(5), O(7), and O(8) of the OPr^i ligands were found to have dual-site disorder. This created dual-site pairs: for O(5), dual sites for C(11)/C(11′), C(12)/C(12′), and C(13)/C(13′) were fixed at 0.7 and 0.3 occupancies for each pair, respectively; for O(7), the dual site for C(17)/C(17′) was fixed at 1/2 occupancy; for O(8), dual-site pairs for C(21)/C(21′) and C(22)/C(22′) were fixed at 1/2 occupancy. Due to the complication of the OPr^i disorder, hydrogens were left off during refinement.

Compound 2a. The OPr^i group of O7 appeared disordered and was modeled by placing 1/2 occupancy of C on each methyl site for the disordered OPr^i ligand. Due to the close proximity of the methyl carbon sites, which yielded unusually distorted thermal ellipsoids, the methyl Cs were refined isotropically. Because of the complication of the OPr^i disorder, hydrogens were left off during refinement; however, the appropriate number of H atoms was included in the formula in the final refinement in order to calculate the correct crystallographic data.

Compound 2b. There are two unique molecules within the unit cell. Both molecules sit on edges of the cell: one molecule straddles the *a*-axis and the other the *c*-axis. There was considerable disorder of the terminal OPr^i ligands, which led to rather large thermal ellipsoids for the methyl carbons.

Compound 3. The ONep molecules were disordered and would not refine anisotropically. Restraints were used to improve the bond lengths of the disordered ONep ligands ($\sigma = 0.04$) that forced all like bonds in a disordered ONep ligand to be the same as like bonds of the other ONep ligands. Due to the disorder of the ONep ligands, Hs were not added to these ligands. Hydrogens were calculated for the DHP and py ligands.

Compound 4a. Several OPr^i groups appeared to have disordered OBu^t ligands superimposed on them and were modeled by placing 2/3 occupancy of C on each methyl site for the disordered ligand. This resulted in a 50 : 50 ratio of OPr^i to OBu^t on each disordered ligand position. It is likely that the OBu^t ligand content is larger than that reported in that it is possible that some of the other OPr^i ligands modeled as fully occupied OPr^i also contained some disordered OBu^t ligand. Due to the complication of the OPr^i/OBu^t disorder, hydrogens were not added to the OPr^i and OBu^t ligands.

Compound 4b. It was noted that all of the terminal ligands (with the exception of the pys) had a great deal of disorder, as it was unclear whether the ligand was OPr^i or OBu^t. Hence, the ligands were refined as possibly being OBu^t or OPr^i by setting occupancies for all the methyl carbons to a reduced value. It was found that the 0.777 occupancy value was sufficient to model the methyl C sites. This allowed for a disordered OPr^i 2/3 of the time and an OBu^t occupying the ligand locations for the remaining 1/3. Due to the severe disorder caused by OBu^t/OPr^i mixing, many of the methyl carbon atoms refined with elongated thermal ellipsoids. These problematic methyl C atoms were instead refined as isotropic. To add additional stability to the refinement, restraints were used to make all C–CH_3 bonds in the OBu^t/OPr^i modeled ligands equivalent. Additionally, all distances between methyl C and neighboring methyl C atoms were restrained so that symmetric appearing ligands would be refined. Due to the complexity of the OBu^t/OPr^i disorder, hydrogen atoms were not added to the structure.

Compound 5. Two py groups were found to have dual-site disorder for N(3) and N(4) atoms. For the N(3) py ligand, two separate orientations were found which created dual-site pairs for C(19)/C(19′), C(20)/C(20′), and C(21) C(21′). For the N(4) py ligand, two separate orientations were also found with the py group which created dual-site pairs for C(24)/C(24′), C(25)/C(25′), and C(26) C(26′). Dual sites for disordered carbons were fixed at 1/2 occupancy and refined anisotropically. Due to the disorder, hydrogen atoms were not added to carbons on the py ligands.

Results and discussion

A recent report[13] details the use of the DHP ligand to link two molybdenum anisylformamidinate species. The DHP ligand was found to act as a bridge between the two metal centers, using the oxygens of the alcohol and the nitrogens of the ring. The synthesis involved the complex metathesis of the Mo anisylformamidinate salt and the NEt_4^+ salt of DHP in acetonitrile. A similar ligand, *S*-methyl thiobarbituric acid (H_2TbSMe), has also been reported in the literature and used in reactions with phenylmercury(II) acetate, affording [$(HgPh)_2$TbSMe].[14] This molecule is asymmetric with two independent [$(HgPh)_2$TbSMe] moieties. In the first molecule, the Hg binds primarily to the N atoms of the TbSMe, whereas in the other, the Hg binds to both the N and O atoms. There are also a number of inter- and intramolecular interactions with the remaining O and the S atoms.

In this study, we have isolated the first $M(OR)_x$ compounds that use the DHP ligand exclusively as a bridge between two metal centers. The following discussion focuses on the synthesis and characterization of **1**–**5**, the structures of which are shown in Fig. 1–5, respectively.

Synthesis

The reactions of the various $M(OR)_4$ with DHP-H_2 were undertaken in toluene following the reaction scheme shown in eqn. 1. Upon mixing the reagents, the DHP ligand proved to be insoluble, forming a yellow slurry. Pyridine (py) was then added and the reaction mixture heated until clear yellow solutions were observed. X-Ray quality crystals of **1**–**5** were isolated by greatly reducing the volume of the reaction mixture and allowing the resulting concentrated solution to sit at glovebox temperatures. For **2**, the isolated material was heated in toluene until dissolution. This results in removal of the coordinated py ligands and allows a closed ring-like structure to be isolated upon cooling to room temperature. Two different sets of unit cell parameters were obtained for this molecule, ascribed to compounds **2a** and **2b**. The mixed ligated species **4a** resulted from the use of impure $Ti(OBu^t)_4$ (99.99%) purchased from Chemat Technology, Inc. Using an equimolar mixture of $Ti(OPr^i)_4$ and $Ti(OBu^t)_4$, formulated as '$Ti(OPr^i)_2(OBu^t)_2$', we isolated an alterative species, **4b**. The central cores of these compounds are identical, but the ratios of OPr^i to OBu^t vary.

Table 2 ^{13}C CP-MAS NMR data for **1**–**4a** and **5**

Compound	^{13}C chemical shift (ppm)
DHP-H_2	171.1, 167.2, 150.2, 91.2 (DHP-H_2)
1	177.4 (DHP), 150.6, 138.5, 124.4 (py), 84.6 (DHP), 78.5, 77.6, 75.9 [O*C*H(CH_3)$_2$], 27.7, 26.3, 23.6, 20.2 [OCH(*C*H$_3$)$_2$]
2	178.2, 149.7, 82.6 (DHP), 80.6, 80.4, 80.0, 79.2, 78.9, 75.6, 74.8 [O*C*H(CH_3)$_2$], 28.1, 27.6, 26.7, 26.3, 25.3, 25.2, 24.8, 24.4, 23.5 [OCH(*C*H$_3$)$_2$]
3	177.4 (DHP), 150.3, 137.8, 123.9, 87.9, 87.1, 86.0 [O*C*H$_2$C(CH_3)$_3$], 73.5 (DHP), 33.9 [OCH$_2$*C*(CH_3)$_3$], 28.0, 27.3, 26.7 [OCH$_2$C(*C*H$_3$)$_3$]
4a	177.3, 150.5 (DHP), 149.8, 137.0, 124.3 (py), 84.3 (DHP), 79.7, 77.9, 77.0, 75.7 [O*C*H(CH_3)$_2$], 50.1 [O*C*(CH_3)$_3$] 32.2 [OC(*C*H$_3$)$_3$], 26.8, 25.9, 24.3, 23.1 [OCH(*C*H$_3$)$_2$]
5	177.8 (DHP), 150.0, 137.6 (py), 125.2 (DHP), 123.7 (py), 87.1 (DHP), 75.1, 74.4 [O*C*(CH_3)$_3$], 34.0, 33.34, 32.7 [OC(*C*H$_3$)$_3$]

Several attempts were made to isolate the DHP derivatives of Ti(OBu^t)$_4$ and Zr(OPr^i)$_4$, but these experiments did not provide X-ray quality crystals. While the resulting powders were fully characterized, it was not possible to unequivocally establish the structures of the derivatives and so these data will not be presented.

The FT-IR spectra of crystals of **1**–**5** reveal the absence of the –OH stretch for DHP, indicating that the reaction was completed. For **1**–**5**, bands due to stretching of the bonds of DHP are readily observed in the range 1615 to 1603 cm^{-1}, which is only slightly shifted from the 1608 cm^{-1} observed for the free DHP-H_2 ligand. Elemental analyses of the bulk material of **1**–**5** often revealed powders with atom contents which were not in agreement with the solid-state crystal structure. This was attributed to the volatility of the bound py. To verify this, solid-state NMR data were collected for each sample.

Single crystal X-ray structures

The DHP ligand acts only as a bridge in each of these compounds, using both the O of the aryloxide and the N of the pyridimine ring. This is similar to what was observed for the molybdenum anisylformamidinate DHP species.[13]

For the OCHMe$_2$ derivatives, two arrangements were noted in the solid state, chair (**1**) and ring (**2**), shown in Fig. 1 and 2, respectively. For both, each Ti is octahedrally (O_h) bound, wherein there are two moieties where the DHP ligand bridges between two 'Ti(OR)$_3$' subunits, forming two M–O–C–N rings. These subunits each bridge a μ-OR to form an '(OR)$_2$Ti(DHP)-Ti(μ-OR)(OR)$_2$' moiety. For **1**, a molecule of py solvent binds to the terminal octahedrally bound Ti metal centers, completing the coordination sphere and forming a chair-like arrangement. For **2**, the bound py is removed from the metal center and no other Lewis basic solvents are available for coordination. Therefore, two previously terminal ORs now act as μ-OR bridging ligands, completing the O_h coordination sphere and thereby forming a ring-like geometry.

The remainder of the molecules (**3**–**5**) adopt the same general structure, [(OR)$_3$M]$_2$(μ_4-DHP) (Fig. 3–5), regardless of the steric bulk of the pendant hydrocarbon chains or metal used. For these compounds, the DHP ligand again, as noted for the subunits of **1**, bridges between the metals using both N and O to bind to the metals. In addition to the DHP and three alkoxides, the metals bind a py solvent molecule to complete their O_h coordination spheres.

The bond distances and angles of these compounds are in general agreement with literature values.[3,5,6,9,11,15–19] For **1**–**4**, (a) the distances were found to be: Ti–OR = 1.79, Ti–(μ-OR) = 2.02, Ti–O$_{DHP}$ = 2.08, Ti–N$_{DHP}$ = 2.26, Ti–N$_{py}$ = 2.30 Å; and for **5**: Zr–OR = 1.92, Zr–O$_{DHP}$ = 2.32, Zr–N$_{DHP}$ = 2.39, and Zr–N$_{py}$ = 2.44 Å; (b) and the angles were found to be: O$_{DHP}$–Ti–N$_{DHP}$ = av. 60.9 (**1**), 61.5 (**2a**), 61.1 (**3**); 60.2° (**4**); O$_{DHP}$–Zr–N$_{DHP}$ = 57.3° (**5**).

NMR spectroscopy

For each sample, a rotor was packed with crystalline material under an argon atmosphere and solid-state CP-MAS NMR spectra obtained. The data collected are listed in Table 2. Due to the large chemical shift anisotropy of the aromatic carbons, numerous spinning side bands are typically observed in the slower speed spectra, while at higher speeds, primarily only the isotropic shifts are observed.

The ^{13}C CP-MAS spectra for each sample reveal the expected DHP and OR resonances. Due to the locked-out rotation of the pendant hydrocarbon chains, several of these spectra have multiple resonances. Free DHP-H_2 is calculated to give rise to peaks at δ 165, 147, and 96 ppm, but the actual resonances were observed at δ 171, 167, 150, and 91 ppm. The doubling of the tertiary carbon is due to packing inequivalancies, demonstrating the complexities of solid-state NMR which result from the absence of the averaging that is observed in solution-state NMR spectra.

For **1** and **3**, only two of the expected three DHP resonances are observed; the third is believed to overlap with one of the bound py resonances, since the other samples (**2**, **4**, and **5**) show all three DHP resonances, with one located close to the py shifts for **4** and **5**. The large number of methyl and methine resonances for **2** are associated with the locked-out OPr^i moieties. The most upfield DHP signal (δ 91 ppm) is further shifted upfield due to the coordination to the metal center, δ 87–84 ppm. From these data, it is readily apparent that the bulk powder is in agreement with the single crystal X-ray structures.

Crystalline samples of **1**–**5** were redissolved in pyridine-d_5 to investigate their solution behavior. The parent solvent was chosen to minimize more complex solution behavior, such as loss of py ligands, which may be observed in alternative solvents such as toluene-d_8. The sample solutions were prepared as concentrated as possible (*i.e.*, a small amount of undissolved material was present at the bottom of each solution). It is unclear as to the nature of **1** due to the symmetry of the molecule. For **2**, there are three methine resonances and six methyl doublets present, along with one set of DHP resonances. This argues for retention of the molecule with locked-out rotation for the symmetry-equivalent OPr^i ligands. This is confirmed by the six methyl and three methine resonances observed in the ^{13}C{^{1}H} NMR spectrum. Additionally, VT-NMR experiments showed no change in the spectrum, indicating that no equilibrium or dynamic behavior is present. For **3**–**5**, only one set of ^{1}H resonances were noted for the DHP ligand. The upfield proton resonance shifts from 6.14 for the protonated DHP-H_3 ligand to the 5.7 to 5.4 ppm range, the downfield proton shows little change in chemical shift and the OH resonance is absent for each sample. There is only one set of resonances for the various pendant hydrocarbon chains of the terminal alkoxides due to rapid dynamic ligand exchange. These data argue for retention of structure in solution for **2**–**5**. Compounds **1**–**5** are not soluble enough to allow for meaningful molecular weight determinations to be undertaken.

Summary and conclusions

A novel family of metal alkoxides has been isolated incorporating the DHP ligand, which was found to only act as a bridge

between two metal centers. For Ti, the smaller $OCHMe_2$ ligand allowed multiple units of '$[Ti(OR)_3]_2(\mu$-DHP)' to form chair (**1**) or ring-like structures (**2**), depending upon whether the py solvent molecules were coordinated or absent. In comparison, the bulkier ONep ligand (**3**) and a mixture of OPr^i and OBu^t (**4**) yielded only dinuclear species. Replacing Ti with the congener Zr yielded **5**, which was found to adopt a dinuclear arrangement. The compounds appear to maintain their structure in solution. The potential use of such an approach as a means for controlled construction of complex precursors to ceramic materials is being explored.

Acknowledgements

The authors would like to thank the Office of Basic Energy Sciences of the Department of Energy for support of this research. Sandia is a multiprogram laboratory operated by Sandia Corporation, a Lockheed Martin Company, for the United States Department of Energy under contract DE-AC04-94AL85000. The authors would also like to thank Dr S. D. Bunge and Mr N. L. Andrews of SNL for their assistance in obtaining the single crystal data.

References

1 M. Y. Turova, E. P. Turevskaya, V. G. Kessler and M. I. Yanovskaya, *The Chemistry of Metal Alkoxides*, Kluwer Academic Publishers, Boston, 2002.
2 D. C. Bradley, R. C. Mehrotra and D. P. Gaur, *Metal Alkoxides*, Academic Press, New York, 1978.
3 D. C. Bradley, R. C. Mehrotra, I. P. Rothwell and A. Singh, *Alkoxo and Aryloxo Derivatives of Metals*, Academic Press, San Diego, 2001.
4 C. D. Chandler, C. Roger and M. J. Hampden-Smith, *Chem. Rev.*, 1993, **93**, 1205.
5 L. G. Hubert-Pfalzgraf, *New J. Chem.*, 1987, **11**, 663.
6 T. J. Boyle, R. W. Schwartz, R. J. Doedens and J. W. Ziller, *Inorg. Chem.*, 1995, **34**, 1110.
7 T. J. Boyle and R. W. Schwartz, *Comments Inorg. Chem.*, 1994, **16**, 243.
8 T. J. Boyle, T. M. Alam, D. Dimos, G. J. Moore, C. D. Buchheit, H. N. Al-Shareef, E. R. Mechenbier and B. R. Bear, *Chem. Mater.*, 1997, **9**, 3187.
9 T. J. Boyle, R. P. Tyner, T. M. Alam, B. L. Scott, J. W. Ziller and B. G. J. Potter, *J. Am. Chem. Soc.*, 1999, **121**, 12104.
10 Personal communication with Prof. William S. Rees, Georgia Institute of Technology, Atlanta, GA, USA, concerning unpublished work.
11 T. J. Boyle, T. M. Alam, E. R. Mechenbeir, B. Scott and J. W. Ziller, *Inorg. Chem.*, 1997, **36**, 3293.
12 The listed versions of SAINT, SMART, XSHELL, and SADABS software are from Bruker Analytical X-Ray Systems Inc., Madison, WI, USA.
13 F. A. Cotton, J. P. Donahue, C. A. Murillo, L. M. Perez and Y. Rongmin, *J. Am. Chem. Soc.*, 2003, **125**, 8900.
14 R. Carballo, J. S. Casas, M. S. García-Tasende, A. Sánchez, J. Sordo and E. M. Vázquez-López, *J. Organomet. Chem.*, 1996, **525**, 49.
15 H. Aslan, T. Sielisch and R. D. Fischer, *J. Organomet. Chem.*, 1986, **315**, C69.
16 T. J. Boyle, T. M. Alam, C. J. Tafoya and B. L. Scott, *Inorg. Chem.*, 1998, **37**, 5588.
17 K. G. Caulton and L. G. Hubert-Pfalzgraf, *Chem. Rev.*, 1990, **90**, 969.
18 J. A. Ibers, *Nature (London)*, 1963, **197**, 686.
19 D. A. Wright and D. A. Williams, *Acta Crystallogr., Sect. B*, 1968, **24**, 1107.